Performance Analysis and Resource Allocation for Intelligent Solar Aware Cellular Base Stations

Sonia Naderi, *Member, IEEE,* Yawen Guo, Colleen Josephson, *Member, IEEE*

***Abstract*—In response to the global climate crisis, solar-powered cellular base stations (BSs) are increasingly attractive to mobile network operators as a green solution to reduce the carbon footprint of networks. However, solar power presents challenges due to its diurnal nature and significant variations in harvestable power due to weather changes. To address these challenges, solar deployments rely on batteries to provide power during the night and periods of low sunlight. Batteries are expensive and have complex environmental considerations, making it desirable to minimize their use at each BS and avoid over-provisioning. Accurate prediction of energy income is essential to minimize the number of Photovoltaic (PV) panels and batteries required while maintaining the quality of service (QoS), achieve a desired energy outage probability, for users.**

This paper introduces an innovative approach to predict energy harvesting by utilizing a novel conditional Long Short-Term Memory (Cond-LSTM) neural network architecture. Compared with standard LSTM and Transformer models, the Cond-LSTM model reduced the normalized root mean square error (nRMSE) by 69.6% and 42.7%, respectively. The proposed approach facilitates an accurate, cost-optimal PV-battery configuration that meets outage probability requirements and aids in site design for regions lacking historical solar energy data. Additionally, we propose a solar-aware cellular communication scheme and user power allocation to enhance QoS via signal-to-noise ratio (SNR) optimization and minimize the probability of energy outages in the cellular system.

Simulation results show the efficiency of our proposed solar aware model in decreasing the overall outage probability of the system and increasing the data throughput of the cellular system. For the same battery configuration, our algorithm achieves 60 percent smaller outage probability and 8 billion bps greater data throughput than a non solar aware approach.

***Index Terms*—Green communications, resource dimensioning, solar energy, base stations, cellular networks**

I. Introduction

The number of mobile network subscribers has been rising rapidly [1], resulting in an increased number of base stations (BSs) and high network energy consumption [2], [3]. The cost of energy is one of the largest operating expenses for mobile network operators [4]. Furthermore, as the Information and Communication Technology (ICT) sector moves overwhelmingly towards significant emissions reduction, the carbon footprint of the energy used to power our mobile networks is becoming a top concern [5]. Powering BSs from locally-generated renewables, such as solar, is drawing increasing interest [3]. In 2014, there were 43,000 BSs around the globe fully or partially powered by onsite renewable generation [6], and as of 2022, that number has grown to more than 70,000 [7]. In addition to decreased energy costs and a lower carbon footprint, locally-generated renewables also improve efficiency by maximizing the amount of useful energy expended. For example, today's grid incurs 10-15% transmission line losses [4], and losses worsen the further towards the edge the consumer is located. Cell towers are often on the far edge, so they suffer steep losses. By placing the solar panels close to the consumer, energy losses are minimized.

Power management in wireless communications has always been a challenging problem [8], [9]. Solar power is a very popular renewable generation option [10]. Solar energy is harvested during the day using photovoltaic (PV) panels, and excess power is stored in batteries to support operations at night or when the sun is occluded. The most important design considerations for solar-powered BSs are the size and number of PV panels, and the number of batteries. Over-provisioning leads to unnecessarily high costs, so operators typically want the smallest number of panels and batteries necessary to provide the desired system performance. A key performance indicator is the system energy outage probability. Outages occur when a BS does not have enough energy to operate reliably. Frequent system outages lead to poor quality of service (QoS) and wasted resources.

Our work aims to introduce a comprehensive framework for optimizing the design and operation of solar-powered cellular base stations (BSs), addressing critical challenges related to energy harvesting, resource allocation, and system reliability.

A. Overview of current state-of-the-art

In a mobile network User Equipment (UE) sends data requests to a BS. The BS retrieves data and provides it to the user in the form of data packets. These data packets are framed into larger data frames and transmitted from the BS to the UE. Allocating radio resources at the BS, i.e., power and spectrum, to multiple users in a single data frame is known as the scheduling and resource allocation (SRA) problem. SRA has been well-studied from a variety of performance perspectives: (1) spectral efficiency, (2) scalability, (3) computational complexity, (4) QoS, (5) fairness, (6) transmission priority, etc. [11]. Our work primarily considers QoS.

1) Markov-based methods: In the body of work that consider solar base stations from the perspective of QoS, many previous studies rely on Markov models [12]. Chamola and Sikdar employed Markov processes to model the energy harvested by PV panels and battery levels to evaluate the outage probability of solar-powered BSs [13], [14]. Gorla and Chamola [15] used Markov processes to estimate the overall battery lifetime for a solar-powered cellular BS with a specified PV panel wattage.

Additionally, other studies [16]–[18] have introduced Markov chains as a common method for predicting solar

radiation and energy harvesting. Markov models are relatively simple to analyze and understand. However, they simplify complex weather patterns into discrete categories, which limits their accuracy. Some studies have attempted to enhance prediction accuracy by applying higher-order Markov chains [19], but this comes at the cost of increased system complexity.

2) Machine learning methods: More recent research uses machine learning methods to predict solar irradiance [20]–[23] and energy harvesting [24]. Long Short-Term Memory (LSTM) models are widely used in machine learning for predicting energy harvesting and have demonstrated notable accuracy [25]–[27]. Ku et al. [28] utilized a Convolutional Neural Networks (CNN)-LSTM model to predict energy states in mobile edge computing systems. Han et al. [29] present a prediction method based on LSTM for the stand-alone photovoltaic/wind/battery microgrid. Transformer models, which are based solely on attention mechanisms, without using convolutional or recurrent layers [30], have emerged since 2019 and demonstrated powerful capabilities across a wide range of modern deep learning applications. Several papers have published applications of Transformer models and hybrid methods in solar energy forecasting, such as [31]–[34].

On the one hand, Transformers can handle long-range dependencies more effectively than recurrent models such as LSTM and can process sequences in parallel, leading to significantly faster computation on GPU/TPU hardware for large datasets [35]. On the other hand, Transformer networks have higher computational complexity compared to LSTMs [36]. These characteristics make them more suitable for large-scale tasks. For smaller or moderate-sized tasks—such as forecasting solar energy—Transformer models consume more resources than an LSTM model with comparable accuracy [37]. Solar-powered systems are resource-constrained environments, making the efficiency of LSTMs attractive. For these reasons, we propose the use of an LSTM variant known as a *conditional LSTM*, or Cond-LSTM, for solar energy harvesting forecasting. Cond-LSTMs introduce an additional layer on top of the traditional LSTM layer to enhance prediction performance. This approach serves as a feature-prior model, in which specific features are integrated to guide the network rather than relying solely on raw input data. The conditional layer can be different for different tasks. The benefits of this feature-prior model are higher prediction accuracy and smaller model size. Cond-LSTM networks been used in melody generation [38] and spoken dialogue systems [39], but to the best of our knowledge, our work is the first to explore Cond-LSTMs for energy harvesting predictions. The detailed architecture of the proposed Cond-LSTM used in our paper is described in Chapter 2. In Section V-B we compare our model's performance against standard LSTMs and Transformers in terms of accuracy and resource consumption.

3) Capacity Scheduling and Power Allocation : Capacity scheduling for power allocation in a solar powered system involves the dynamic management of the available battery capacity to meet energy demands. This process includes predicting energy input from photovoltaic (PV) panels, monitoring the battery's state of charge, and efficiently, fairly, and adaptively allocating energy based on solar energy generation and consumption patterns. In addition, it prioritizes the distribution of energy to critical functions when energy availability is restricted [40], [41]. It is possible to use AI/ML methods to facilitate capacity scheduling. For example, [42] uses deep reinforcement learning (DRL) for capacity scheduling in PV-battery systems, optimizing the storage and usage of solar energy. Capacity scheduling focuses on managing energy storage in PV-battery systems for arbitrary loads, and usually assumes connectivity to the larger power grid, allowing users to sell excess capacity to municipal energy providers. The scope of this paper focuses on standalone solar powered base stations, which are often too remote to be connected to the power grid. However, in contexts where a BS is solar powered but is also connected to the grid for backup power, capacity scheduling can be considered a complementary technology to the problem of mobile network power allocation.

Mobile network power allocation is the strategic distribution and management of power resources across BSs and communication channels within a network, with the key objectives of ensuring ample signal quality for users, enhancing system capacity, and curbing interference. Practical power allocation involves assigning power to individual BSs and communication channels to ensure each user receives sufficient signal quality. This allocation improves end-user signal quality, thereby elevating QoS and enabling higher data rates. In the context of solar base stations, ensuring power allocation consistency is essential for reliable service, preventing dropped calls and maintaining network adaptability to fluctuating user demands and weather conditions. Another important role of power allocation is optimizing energy efficiency, which is especially crucial for solar-powered BSs, as minimizing energy usage within solar-powered network prevents power shortages at the BS during inclement weather [43].

There is a rich body of work looking at power allocation algorithms. [44] investigates communication within an uplink cellular network and develops a spectrum and power allocation strategy to maximize the total average achievable rate while adhering to the constraints of a target outage probability. [45] explore the role of machine learning in power allocation by using a novel reinforcement learning (RL) algorithm combined with a pointer network (PN) to optimizing spectrum efficiency for device-to-device (D2D) communications in cellular networks. In fact, many works focus on D2D communications, including [46]–[48].

Vallero et al. [49] propose a machine learning-based approach for optimizing energy usage in the Radio Access Network (RAN) to reduce carbon emissions. Their focus is on operational efficiency across a broad RAN, utilizing predictive models to manage energy consumption. While Vallero et al. emphasize energy optimization in a broader RAN context, our work specifically addresses the energy management of macro cellular base stations (BSs) powered by solar energy. We introduce a Cond-LSTM model for solar energy harvesting prediction, which achieves superior accuracy compared to Markov, LSTM and Transformer models, as demonstrated in our results. Additionally, we combine this predictive model with a solar-aware resource allocation strategy, which is not addressed in Vallero et al.'s study. Piovesan et al. [50] propose

a machine learning approach for joint load balancing and energy sharing among renewable-powered small BSs, focusing on distributed energy management. While Piovesan et al. concentrate on small-scale BSs and energy-sharing techniques, our work is tailored for macro BSs, which have significantly higher energy demands and operational complexities. Our framework integrates solar energy prediction and resource allocation, providing a holistic solution for PV-powered macro BSs. Unlike their energy-sharing model, we optimize the system for single BS scenarios with cost-optimal provisioning of PV panels and batteries, maintaining 99.9 percent uptime.

The studies above are primarily focused on increasing the QoS of cellular networks by efficient power and resource management and assume a reliable and relatively unconstrained supply of power. To the best of our knowledge, there is no work that optimizes resources considering the unique needs of on-site renewable energy harvesting. We propose a model for power allocation of solar-powered BSes that is informed by predictions of how much power can be harvested. Our work uniquely combines Cond-LSTM-based solar energy prediction with a solar-aware power allocation strategy to optimize the operation of macro BSs. While the referenced studies focus on different scales (RAN-level, small BSs) or specific aspects (storage management, load balancing), our study holistically addresses the unique challenges of macro BSs powered by renewable energy, achieving higher accuracy and operational efficiency metrics.

B. Contributions of This Work

This paper introduces a comprehensive framework for optimizing the design and operation of solar-powered cellular base stations (BSs), addressing critical challenges related to energy harvesting, resource allocation, and system reliability. The specific contributions of this work are as follows:

1) **Accurate Solar Energy Prediction:** We propose a Conditional Long Short-Term Memory (Cond-LSTM) model tailored for predicting solar energy harvesting. The model significantly improves prediction accuracy compared to Markov, LSTM and Transformer models. As demonstrated in Section 5, our approach achieves a normalized root mean square error (nRMSE) of 0.78%, outperforming Markov (21.24%), LSTM (2.38%) and Transformer (1.48%) models.
2) **Optimization of Resource Allocation:** A novel solar-aware power allocation strategy is developed to maximize network performance by enhancing signal-to-noise ratio (SNR) while minimizing energy outages. Our results in Section 5 highlight a 60% reduction in energy outage probability compared to non-solar-aware strategies.
3) **Enhanced Network Throughput:** By leveraging solar-aware optimization, the proposed model achieves an 8 billion bps improvement in network throughput compared to non-solar-aware methods, as shown in Fig. 11.
4) **Cost-Optimal Provisioning:** Our framework determines the minimum number of PV panels and batteries required to maintain 99.9% uptime while minimizing costs. The optimization uses Mixed-Integer Linear Programming (MILP) to balance energy demands and resource provisioning effectively.
5) **Generalizability Across Regions:** The Cond-LSTM model demonstrates strong generalization across diverse geographical regions, enabling accurate predictions even for locations lacking historical solar energy data. This capability ensures broader applicability of the proposed framework.

These contributions collectively advance the state-of-the-art in the design and operation of solar-powered cellular BSs, enabling efficient energy management and enhanced quality of service in green communication networks.

The remainder of this paper is organized as follows. Section 2 presents the system model and problem formulation. Performance analysis for a single cell (one BS) scenario is presented in Section 3. Section 4 focuses on energy outage performance analysis for Non-Solar vs. Proposed Solar-Aware models. Simulation setup and results are presented in Section 5. The paper is concluded in Section 6, and future directions are discussed in this section.

II. System Model and Problem Formulation

A. System Model

The proposed system model, as depicted in Fig. 1, focuses on utilizing PV panel to power a BS in the context of a 5G network. This system captures energy from sunlight using PV panels, which, together with batteries, power the BS. Under sunny conditions, the PV panels generate enough energy to not only directly power the BS but also store any excess energy in the batteries. Conversely, during nighttime or cloudy days when the PV panels cannot produce sufficient energy, the stored energy in the batteries is used to maintain the BS's operations. The system comprises several components: PV panels for energy harvesting, a battery bank for energy storage, an energy management unit to manage energy storage and consumption, and a cellular BS to support energy consumers or loads. Fig. 1 presents the high-level architecture of a solar-powered BS. This system harnesses energy from sunlight through PV panels, which, in conjunction with batteries, powers the BS.

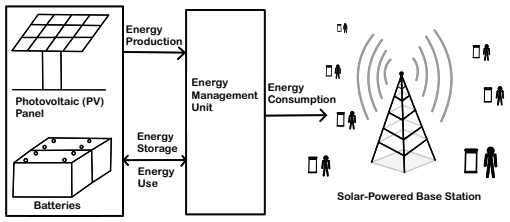

Fig. 1. Architecture of the Solar-Powered BS System.

To ensure continuous operation, the system employs a mechanism to balance energy supply and demand. If the energy harvested by the PV panel is insufficient to meet the consumption requirements, energy can be extracted from the batteries. Conversely, if the harvested energy exceeds the consumption needs, the excess energy is stored in the batteries for the later use.

In the system modeling process, BS load, harvested solar energy by the PV panel, and battery levels are all modeled.

TABLE I
HYPERPARAMETERS APPLIED FOR COND-LSTM AND LSTM.

Hyperparameter	LSTM	Cond-LSTM
Activation	Dense	Dense
Input	All the Features	Feature "DHI" and other features
Loss	MSE	MSE
Optimizer	Adam	Adam

Furthermore, the energy outage at the BS is modeled as an event occurring when the charge level of the BS batteries falls below a discharge threshold. In such a scenario, the batteries are disconnected from the BS and there is an outage event.

B. Structure of an off-the-grid BS

Sub-parts of a modern BS are as follows:

- **Power Amplifier (PA):** Amplifies the signal to be transmitted, boosting its strength for effective communication.
- **Cooling System:** Preventing overheating and ensuring optimal performance.
- **Edge Compute:** Provides computing capabilities at the edge of the network, enabling real-time processing of data and reducing latency.
- **Antenna System:** Transmits and receives radio frequency signals, facilitating communication with user devices.
- **Baseband Processor:** Handles signal processing tasks, including modulation, demodulation, and error correction.
- **Digital-to-Analog Converter (DAC):** Converts digital signals into analog signals for transmission through the antenna.
- **Analog-to-Digital Converter (ADC):** Converts incoming analog signals, received by the antenna, into digital signals for further processing.
- **Solar Panels:** Harness solar energy to generate electrical power for the BS, contributing to sustainability.
- **Batteries/Power Management System:** Stores excess energy generated by renewable sources (e.g., solar panels) and manages power distribution to ensure continuous operation, even during periods of low energy generation.

C. Energy Harvesting Models

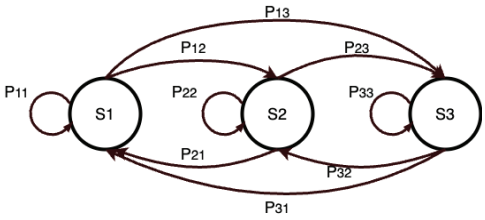

Fig. 2. The Markov Chain of the Solar Power Harvesting Model corresponding to transition matrix defined in [14].

Energy harvesting models play an important role in our solar-aware system, as they enable both one-time provisioning of infrastructure such as solar panels and batteries, as well repeatedly predict solar energy income for the power allocation scheme (see Sec. III). Due to frequent inferences in the power allocation algorithm, the model must be resource efficient.

Our energy harvesting model assumes the scenario where a single macro base station is powered by its own dedicated battery bank. This is because our work focuses on macro base stations, which are assumed to have relatively wide geographic separations, making it impractical to share a battery bank among multiple base stations. Macro BS have high transmission power (about 40W for devices with bandwidth of 20MHz), while micro BS have lower transmission power (typically a few hundreds milliwatts to a few watts) [51]. Traditional LSTM models exhibit satisfactory performance in predicting harvesting energy for micro systems but encounter limitations with macro systems. Transformer models achieve slightly higher accuracy than LSTM [52] but need more calculation resource consumption. Motivated by the challenge of enhancing solar energy prediction accuracy for macro base stations, we introduce the Cond-LSTM model to significantly improve prediction accuracy while having a smaller model size. Specifically, we construct a conditional neural network tailored to solar activity patterns. This is crucial because, for high-capacity PV panels, data during sunlight hours display significant variability compared to other times. Segregating predictions for non-sunlight hours into a separate neural network diminishes data variability and improves data smoothness, thereby facilitating more accurate forecasting. The inputs we are using include time information (Month, Hour), Direct Normal Irradiance (DNI), Diffuse Horizontal Irradiance (DHI), Global Horizontal Irradiance (GHI), Dew Point, Temperature, Pressure, Humidity, Wind Direction, Wind Speed, and Surface Albedo. Differing from a traditional LSTM, our model instead divides the inputs into two parts. Inputs with selected feature DHI are fed into a self-defined lambda layer, while other features are fed into the LSTM model. DNI, DHI, and GHI are three key features most closely related to solar activity. While DNI is strongly influenced by the angle of sunlight and approaches zero during sunrise and sunset, we consider DHI, which is more associated with diffuse radiation, as the input for the lambda layer. GHI, encompassing both DNI and DHI, could also be used for the lambda layer, but we allocate it to the LSTM layer to aid in prediction. The output of lambda layer will decide if we will accept the outputs from LSTM layer. The proposed Cond-LSTM is shown as Fig. 3. Table I displays the hyperparameters of LSTM and Cond-LSTM, with the majority kept consistent to ensure a fair comparison, except for a few essential modifications necessitated by the model construction. Both models are single-layer LSTM/Cond-LSTM architectures containing one dense layer.

We utilize 21 years of statistical weather data provided by the National Renewable Energy Laboratory (NREL) [53], comprising hourly solar irradiance data for specific locations. The weather data is then processed through PySAM of the System Advisor Model (SAM) Software Development Kit [54] to generate the hourly energy output of a PV panel with a specified rating. This serves as the ground truths for our evaluations. Although we evaluated only four typical locations in different climate zones across the United States, the generalization evaluation in this paper demonstrates that the proposed model, with stable and high accuracy, effectively learns the relationship between weather and solar harvesting. This model can be generalized to other climate zones without retraining and still achieve high prediction accuracy when local weather data is provided.

In addition to AI/ML-based modeling, we also compare our results against a three-state first-order Markov process

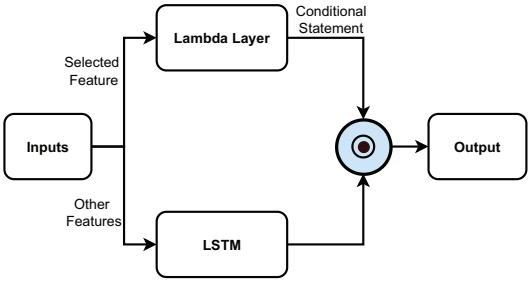

Fig. 3. Proposed Cond-LSTM Model.

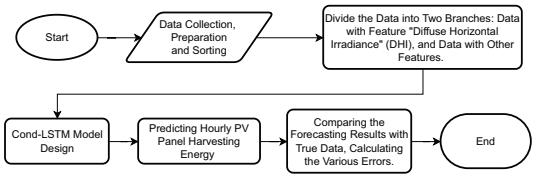

Fig. 4. Flow Chart of Cond-LSTM Model.

described by [14]. Similarly to [14], the weather is categorized into three states: "bad weather (S1)", "not good weather (S2)", and "good weather (S3)". For each month, daily harvesting patterns were calculated by the mean harvesting value of that month in 20 years. Then the thresholds of each day types was determined by the different solar harvesting/irradiance level (reflected as the different percentage in the boxplot, we defined them as "$\leq 50\%$", "$50\%-75\%$" and "$\geq 75\%$" in this paper). Next, we marked those days for different day types according to the thresholds. The transition probability was calculated by 20 year's statistical data of daily solar harvesting. And a transition matrix showing the probabilistic relationship of sub-patterns created accordingly. Different transition matrices are calculated for different months. Fig. 2 illustrates the Markov chain of the harvesting model.

In the Markov model, 20 years of data were used to compute the transition matrices for different months, with an additional year of data dedicated to verifying accuracy. For the LSTM, Transformer and Cond-LSTM models, the dataset is divided into training data (18 years), validation data (2 years), and testing data (1 year). The Cond-LSTM model introduces a conditional neural network architecture designed to process the DHI feature in conjunction with other inputs, effectively distinguishing between non-sunlight hours (with zero harvesting) and sunlight hours. It incorporates LSTM and Dense layers for predictive tasks. Cond-LSTM is applied to the RobustScaler normalization to enhance neural network performance, while we found that LSTMs and Transformers perform better with MinMaxScaler. Furthermore, the training process of all LSTM, Transformer and Cond-LSTM is optimized through the utilization of EarlyStopping, ModelCheckpoint, ReduceLROnPlateau, and a bespoke LearningRateScheduler, all contributing to improved training efficiency and model accuracy. Fig. 4 illustrates the process flow for predicting energy harvested by PV panels using the Cond-LSTM model.

D. Traffic Model

To highlight the practical relevance of our model, we have based our power consumption framework on recent 5G data. Our traffic model utilizes generative normalized traffic data [55], trained on empirical data, and this data has been adjusted to match 5G power consumption figures reported by Huawei [56]. According to Huawei, the power requirements for the Remote Radio Unit (RRU) and Baseband Unit (BBU) at each site exceed 11.5 kilowatts. In our model, we assume a peak power consumption of 11.5 kilowatts for a 5G BS, with approximately 47 percent of this power allocated to the cooling system [57]. The remaining power consumption is calculated using the formula [58]:

$$P_{bs} = \frac{(N_S \times N_{Tx})(\frac{P_{Tx}}{\eta_{PA}} + \frac{P_{BB}}{\eta_{BB}} + \frac{P_{RF}}{\eta_{RF}})}{(1-(c_4+\epsilon_4 n))(1-(c_5+\epsilon_5 n))(1-(c_6+\epsilon_6 n))} \quad (1)$$

where the P_{Tx}, P_{BB}, and P_{RF} are the ideal power consumption for the power amplifier, baseband unit, and transceiver, respectively. They were taken as $P_{Tx} = 500W$, $P_{BB} = 100W$, and $P_{RF} = 100W$. The efficiency η of these parameters depends on the number of connections n (load), as follows: $\eta_{PA} = c_1 - \epsilon_1 n$, $\eta_{BB} = c_2 - \epsilon_2 n$ and $\eta_{RF} = c_3 - \epsilon_3 n$ respectively, where ϵ_i $(i = 1, 2, 3)$ is a coefficient for efficiency that varies with load n for power amplifier, baseband unit and transceiver devices respectively, and c_i $(i = 1, 2, 3)$ represents the corresponding part of the efficiency that is not load-dependent. $\sigma_R = c_4 + \epsilon_4 n$, $\sigma_{DC} = c_5 + \epsilon_5 n$ and $\sigma_{COOL} = c_6 + \epsilon_6 n$ are the loss factors due to rectification, regulation, and cooling, respectively. All the efficiency and loss factors above are between 0 and 1. The parameter ϵ_i is contingent upon the hardware design and specifications of the device and is considered negligible unless the load approaches the magnitude of 10^5–10^6. Peak load is around 14000, so variation of efficiencies with the load is very weak, with all the ϵ_i were taken as 10^{-7}. The efficiencies were taken as $c_1 = 0.75$, $c_2 = c_3 = 0.8$, $c_4 = 0.65$, $c_5 = 0.15$, which we take the same parameters as the article [58]. c_6 is set to be 0.47 according to [57]. Each base station typically has 3 hexagonal sub-sectors (thus $N_S = 3$) and we assume every antenna is deployed for 10,000 devices as in [58]. So the number of antennas for each sub-sector is $N_{Tx} = \frac{n}{10^4}$. The auxiliary power is neglected because of its independence of the load.

E. Sizing the PV Panels and Battery

PV Panel: Numerous common PV panel sizes are available. In our model, we select a configuration of 72 cells which measures approximately 1 meter × 2 meters [1].

Battery Bank: Lithium-ion batteries are particularly suitable for photovoltaic standalone systems due to their reliability, modularity, and durability.

Optimal Sizing: Determining the optimal number of PV panels and batteries is essential for the construction of a solar-powered BS. It requires consideration of not only the tolerable outage probability but also the need to minimize costs. To determine the optimal sizing, we assess the residual energy from the previous hour in the batteries, $E_{Battery}(i-1)$, plus the energy harvested in the current hour, $E_{harvest}(i)$, comparing this sum to the current hour's energy consumption, $E_{consume}(i)$, where i denotes the hour in question. We assume

[1]For both PV panels and batteries, the prices are drawn from the options available in an online retailer as of Mar 19th, 2024. For cost comparisons, we use Mission Solar 430W monocrystalline MIN-MSE430SX9Z ($244) and the Generac PWRcell 3.0kW Lithium-Ion Battery Module G0080040 ($2093).

that that all Lithium-Ion batteries are fully charged prior to the BS's operation, with each battery's capacity, C_B, being 3.0 kWh. To prevent battery damage due to excessive discharge, we simply set the minimum state-of-charge (SoC) as 20%, which means a lower limit is established at 20% of a battery's capacity [59]. Consequently, the BS operates normally if $m \cdot E_{Battery}(i-1) + n \cdot E_{harvest}(i) - E_{consume}(i) > 20\% \cdot m \cdot C_B$, where m is the number of batteries and n is the number of PV panel modules. Conversely, an outage occurs if $m \cdot E_{Battery}(i-1) + n \cdot E_{harvest}(i) - E_{consume}(i) < 20\% \cdot m \cdot C_B$. In the sizing model, it is assumed that a maximum of one hour of outage is permissible over a span of approximately a month (671 hours), which corresponds to 99.9% uptime. Given this threshold for outage tolerance, the goal is to ascertain the necessary quantities of PV panel and battery modules to minimize overall costs. In this analysis, installation and maintenance expenses are not considered. The constrained optimization problem is described below:

Objective Function:

$$\text{Minimize cost} = n \cdot \texttt{PV\_cost} + m \cdot \texttt{Battery\_cost} \quad (2)$$

Subject to: Initial Battery Level:

$$E_{\text{Battery}}(0) = m \cdot C_B \quad (3)$$

Available Energy:

$$E_{\text{avail}}(i) = E_{\text{Battery\_trim}}(i-1) + n \cdot E_{\text{harvest}}(i) - E_{\text{consume}}(i) \quad (4)$$

Outage Constraints:

$$E_{\text{avail}}(i) \geq 0.2 \cdot m \cdot C_B + \varepsilon - M \cdot \text{outage\_indice}(i) \quad (5)$$

$$E_{\text{avail}}(i) \leq 0.2 \cdot m \cdot C_B + \varepsilon + M \cdot (1 - \text{outage\_indice}(i)) \quad (6)$$

Battery Energy Update:

$$E_{\text{Battery}}(i) = E_{\text{avail}}(i) + E_{\text{consume}}(i) \cdot \text{outage\_indice}(i) \quad (7)$$

Trimmed Battery Constraints:

$$E_{\text{Battery\_trim}}(i) \leq \min\left(E_{\text{Battery}}(i), m \cdot C_B\right) \quad (8)$$

Battery Capacity Constraints:

$$E_{\text{Battery}}(i) \leq m \cdot C_B \quad (9)$$

$$E_{\text{Battery}}(i) \geq 0 \quad (10)$$

Total Outage Constraint:

$$\sum_{i=1}^{\text{len\_data}} \text{outage\_indice}(i) \leq 1 \quad (11)$$

A Mixed-Integer Linear Programming (MILP) approach with big-M method is used to solve this problem, where M is a sufficiently large constant to force a constraint to be either active or inactive. Taking the Iowa (IA) region as an example, for 99.9% uptime, harvesting projections are calculated via Cond-LSTM, whose output is used in the MILP to solve the optimal solutions for the number of solar panels and batteries.

A Mixed-Integer Linear Programming (MILP) approach with big-M method is used to solve this problem, where M is a sufficiently large constant to force a constraint to be either active or inactive. $outage\_indice(i) = \{0, 1\}$, where 1 means an outage happen and 0 means no outage happen. Taking the Iowa (IA) region as an example, for 99.9% uptime, the optimal solutions for solar panels and storage batteries are calculated via Cond-LSTM are 47 and 22 respectively. Fig. 5 presents the data on energy consumption versus energy availability extracted from a 48-hour period surrounding an outage occurring under this configuration. As the day progresses, the battery bank is fully charged to a capacity of 66 kWh, which corresponds to 52.8 kWh of usable capacity due to the system policy of never draining the batteries below 20%.

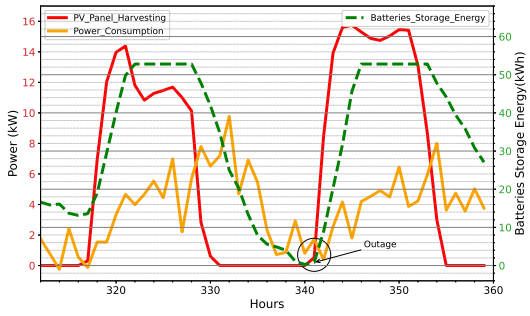

Fig. 5. Outage of an example BS with energy consumption, PV panels harvesting energy and batteries storage energy across 48 hours. Batteries storage energy are shown as zero when the 80% of the batteries drained, due to the 20% lower limit.

III. Resource Allocation Analysis

For a BS providing service to users at location x, the data rate $c(x)$ is derived from the Shannon-Hartley theorem and expressed as [60]:

$$c(x) = BW \cdot \log_2(1 + \text{SNR}(x)) \quad (12)$$

with BW being the total bandwidth of BS and $\text{SNR}(x)$, the signal-to-noise ratio, is calculated as

$$\text{SNR}(x) = \frac{g(x)P(x)}{\sigma^2} \quad (13)$$

where $g(x)$ signifies the channel gain from BS to the user at x, accounting for shadowing and path loss, $P(x)$ is BS transmission power, σ^2 is the noise power which its unit would be in watts (W) since $P(x)$ is in watts and $g(x)$ is dimensionless. This paper assumes that precise channel state information (CSI) is available, which can be estimated from the terrain topology and site surveys. While the assumption of having precise channel gain information from terrain topology and site surveys is useful for theoretical and simulation purposes, its real-world application can be limited by environmental complexity, technological capabilities, and dynamic changes. It's more realistic in controlled or less complex environments and serves as a good starting point for initial network design and simulation studies. In practice, ongoing adaptation and updates to channel gain information are necessary for optimal network performance.

For simplicity, we use the average SNR of each channel from a BS to a user during 24 hours to compute the BS's offered data rate at x. We define the load ρ for BS as the proportion of time it is occupied with serving requests.

A. Objective User Power Allocation Optimization Problem

Our goal is to optimize the utilization of sustainable energy sources accessible to the BS with the intention of enhancing the SNR for each communication within the network. Concurrently, it is imperative to prevent any lapses in energy supply at the BS. Therefore, we present an optimization problem that aims to elevate the cumulative SNR throughout the network over the course of the day, contingent on the solar energy harnessed by the BS. This problem is structured as follows:

$$\begin{aligned} \text{Maximize} \quad & \sum_{i=1}^{24} \int_R \text{SNR}(x)\, dx \\ \text{subject to} \quad & \sum_{i=1}^{24} L_i \leq E \\ & 0 \leq \rho_i \leq 1 \quad \text{for all } i, \end{aligned} \tag{14}$$

where L_i indicates the power usage of the BS during hour i, and E signifies the allocation of green energy for the BS throughout the day.

In this work, L_i includes both the power allocated for user transmissions and the operational power required for the BS's core functionality, such as cooling and control systems. The total BS power consumption is influenced by the transmission power allocation, as well as the efficiency of the power amplifiers and other supporting hardware. The optimization framework ensures that the relationship between transmission power and total BS power consumption is accounted for, while adhering to the green energy constraints. This approach guarantees that the BS operates within its available energy budget, optimizing the cumulative SNR across the network while preventing any interruptions in energy supply. The traffic demand is assumed to be evenly distributed among the users, with stochastic variations accounted for over time. The optimization is based on the prediction of solar energy availability and the expected traffic demand throughout the day. The BS operational power is considered constant, while user transmission power depends on the traffic demand and channel conditions. We should mention that, the power allocated to each user is closely tied to the BS's total transmission power, which is distributed based on user needs and channel conditions. Factors like connection quality, user distance, and network traffic influence this allocation. Users with weaker signals or farther from the BS require more power, while others need less. The allocation process optimizes transmission power to enhance network performance while adhering to energy constraints, especially in solar-powered systems, ensuring reliable communication without energy overuse or outages.

Determining whether an optimization problem is convex involves examining the objective function and the constraints to see if they meet the criteria of convexity.

For the sake of illustration, we choose 5 users. This specific number allows us to demonstrate the key concepts and evaluate the performance of the proposed system without overcomplicating the analysis. By selecting 5 users, we can effectively showcase the dynamics of power allocation and system performance under realistic, yet manageable, conditions. Additionally, this choice aligns with common scenarios in wireless communication research, where a moderate number of users is used to balance computational feasibility and practical relevance. While the number of users could vary in real-world deployments, the insights gained from this analysis remain applicable and scalable to larger systems.

In the simulation section, the optimization problem is aimed at determining the optimal power allocation to each of the 5 users over a 24-hour period, with decisions made every second. The outcome of the optimization provides the power values assigned to each user at each interval, ensuring that the cumulative SNR across the network is maximized while satisfying the energy budget constraints.

B. Optimization Problem Solving Approach

Problem Formulation: Our objective is to maximize the cumulative Signal-to-Noise Ratio (SNR) over a specified period within a cellular network. This involves optimizing the power allocation to multiple users across several time intervals while adhering to specific constraints. The cumulative SNR is computed using the Shannon-Hartley theorem, which captures the logarithmic relationship between channel capacity and SNR. The optimization aims to achieve a balance between maximizing network throughput and maintaining feasible power usage.

The decision variables in this problem are the power allocations (P) to each user in each interval. The constraints ensure that power allocations remain within the available energy budget and do not exceed the maximum allowable transmission power for each user. The objective function explicitly incorporates these elements, as described in Eq. 14.

Parameters and Variables: The key parameters and variables include the number of users (**numUsers**) in the network and the number of intervals (**numIntervals**) considered during the optimization period. For instance, if the optimization period spans 24 hours, setting **numIntervals** to 17280 implies that power allocation decisions are made every 5 seconds, resulting in a total of 17280 intervals.

Additional parameters include:

- Stochastic channel gains for each user (g), representing the quality of the communication channel.
- Noise power σ^2, which impacts achievable SNR.
- Total available bandwidth (**BW**).
- Maximum allowable power for transmission (**P_max**).
- Total energy budget for power allocation across the optimization period (**Energy Budget**).

Objective Function: The objective function maximizes the total SNR across all users and intervals. For each user in a given interval, the SNR is defined as a function of the allocated power (P), channel gain (g), and noise power (σ^2):

$$\text{Maximize} \quad \sum_{\text{all intervals}} \sum_{\text{all users}} \log_2 \left(1 + \frac{g \times P}{\sigma^2}\right) \tag{15}$$

This formulation aligns with the practical goal of enhancing network throughput while ensuring efficient resource utilization. The logarithmic term captures the diminishing returns of increasing power allocation due to the noise-limited nature of wireless channels.

Optimization Approach: To solve this optimization problem, we use MATLAB's nonlinear programming solver, `fmincon`. The solver is provided with:

1) **Objective Function**: The negated version of the above function to facilitate minimization, as `fmincon` is a minimization solver.
2) **Constraints**:
   - **Linear Constraints**: Bounds on power allocations to ensure $0 \leq P \leq$ **P_max**.

- **Nonlinear Constraints**: The energy budget constraint, which ensures that the total energy consumed across all intervals does not exceed the available budget (**Energy Budget**).

The optimization process iteratively adjusts the power allocations, evaluating the objective function and checking the constraints at each step. The solution provides an optimal set of power allocations that maximizes the cumulative SNR while satisfying all constraints.

This approach ensures that the practical requirements described in Section 3.2 align with the mathematical formulation in Eq. 14. The effectiveness of this method in reducing system outages and improving cellular communication throughput is demonstrated in the simulation results section.

IV. Energy Outage Performance Analysis for Non-Solar vs. Proposed Solar-Aware Models

In the optimization problem and simulations discussed so far, we are allocating power to individual users in a cellular communication network. The allocated power serves to enhance the SNR, which is essential for delivering high-quality communication services. It also plays a key role in minimizing the noise throughout the network, ensuring efficient and reliable performance. The optimization problem aims to distribute power resources strategically across users and BSs to achieve these objectives.

In the context of cellular communication networks, allocating power to a user refers to distributing the available power resources among the transmission chains associated with individual users. The power allocation is typically performed at the transmitter chain of the BSs or access points. It involves determining how much power each user's transmission chain should use during a given interval. The goal is to achieve efficient utilization of the available power budget, considering factors such as channel conditions, interference, and noise. Our energy outage algorithm considers energy dynamics throughout the day and operates on a per-second basis.

A. Energy Outage Decision Algorithm Model:

TABLE II
Variable Definitions

Variable	Description
$E_{\text{harvested}}(t)$	Energy harvested by the solar panel at time t.
$E_{\text{consumed\_day}}(t)$	Energy consumed by the BS during the day at time t.
$E_{\text{excess\_day}}(t)$	Excess energy stored in the battery during the day at time t ($E_{\text{harvested}}(t) - E_{\text{consumed\_day}}(t)$).
$E_{\text{threshold-min}}$	Minimum battery level threshold for nighttime operation.
$E_{\text{threshold-max}}$	Maximum battery level threshold.
$E_{\text{consumed\_night}}(t)$	Energy consumed by the BS during the night at time t.
$E_{\text{available}}(t)$	Energy available in the battery at time t.
$E_{\text{outage}}(t)$	Energy outage indicator at time t.

Energy Outage Decision Algorithms in non-solar prediction model during day and night time are implemented in Fig. 6 and Fig. 7. Variable definitions are in Table II. The decisions of how to allocate power will depend on whether or not the system is actively harvesting or subsisting on battery (i.e. daytime vs. nighttime). During the night, we must budget power consumption such that the battery does not completely drain. If the battery drains below some threshold, then we are unable to service users, and this is considered an outage.

During the day, we need to build up battery reserves for nighttime operations, as well as serving the daytime user demands. During nominal operations, there is enough incoming energy to satisfy all the user demand and also charge the battery at some minimum rate needed to meet the a target threshold before sunset. However, if the charge rate will not allow the threshold to be met, then the system must instead temporarily reduce power consumption (e.g, reduce overall transmit power). In the most dire case, the transmit power is as low as possible, but the battery is still not charging. There are two possible choices here: i) begin to drain the battery to satisfy users now, at the expense of night users, ii) incur a daytime service outage to preserve the quality of nighttime service. The best choice will depend on the typical traffic patterns the BS experiences, but for simplicity, we will prioritize daytime users at the cost of night service under these circumstances. During extreme weather (e.g. almost no sunlight all day) it may be possible for the battery to drain fully during the day causing a daytime outage.

*1) **24-Hour Operation Loop in Non-Solar Aware Prediction Model:**:* During the daytime, the algorithm focuses on managing the BS's operation based solely on the energy currently stored in the batteries and energy demands at the current time, t. For a given time t, the solar income is first used to supply the BS's current power draw. Any excess energy after servicing the BS needs is stored into the battery.

If this excess energy is positive, indicating an energy surplus, it is stored in the battery for later use. In cases where the excess energy is negative, indicating an energy deficit, the algorithm takes precautionary measures to avoid further depletion of the battery. It sets the excess energy to zero to prevent negative values and then checks if the remaining energy in the battery, coupled with predicted incoming energy, is sufficient to sustain BS operations. If so, the BS continues operating; otherwise, an outage state is triggered to prevent system failure due to insufficient energy supply.

During the nighttime, when solar energy harvesting is not available, the algorithm manages the BS's operation based solely on the energy stored in the battery. It ensures that the BS operates within the constraints of the available energy to prevent system instability or failure. The algorithm first checks if the available energy in the battery is sufficient to meet the energy consumption demands of the BS during the night. If so, the BS operates normally. In cases where the available energy is insufficient, either due to high energy demand or low battery levels, the algorithm triggers an outage state to prevent system overload and ensure the integrity of critical functions. Additionally, if the available energy falls below a predefined threshold, indicating a critical battery level, an outage state is also initiated to prevent further depletion of the battery and preserve system functionality.

*2) **24-Hour Operation Loop in Proposed Solar Prediction Model:**:* During the daytime, the algorithm manages the operation of the BS in response to varying levels of harvested solar energy and battery state. It follows a series of steps to ensure

Algorithm 1 Daytime Operation (Non-Solar-Aware)

Input: $E_{\text{harvested}}(t)$, $E_{\text{consumed\_day}}(t)$, $E_{\text{available}}(t)$, $E_{\text{threshold-max}}$
Output: $E_{\text{excess\_day}}(t)$, Battery status, $E_{\text{outage}}(t)$
Calculate $E_{\text{excess\_day}}(t) = E_{\text{harvested}}(t) - E_{\text{consumed\_day}}(t)$.
if $E_{\text{excess\_day}}(t) \geq 0$ **then**
  Store excess energy in the battery.
else
  Set $E_{\text{excess\_day}}(t) = 0$ (to avoid negative excess energy).
  if $E_{\text{available}}(t) - E_{\text{threshold-max}} \geq E_{\text{consumed\_day}}(t)$ **then**
    Operate normally.
  else
    Set $E_{\text{outage}}(t) = 1$.
  end if
end if

Algorithm 2 Nighttime Operation (Non-Solar-Aware)

Input: $E_{\text{available}}(t)$, $E_{\text{consumed\_night}}(t)$, $E_{\text{threshold-min}}$
Output: $E_{\text{outage}}(t)$
if $E_{\text{available}}(t) \geq E_{\text{consumed\_night}}(t)$ **then**
  Operate the BS during the night.
else
  if $E_{\text{available}}(t) < E_{\text{consumed\_night}}(t)$ **or** $E_{\text{available}}(t) < E_{\text{threshold-min}}$ **then**
    Set $E_{\text{outage}}(t) = 1$.
  end if
end if

Algorithm 3 Daytime Operation (Solar-Aware)

Input: $E_{\text{harvested}}(t), E_{\text{harvested}}(t+1), \ldots, E_{\text{harvested}}(t+x)$, $E_{\text{available}}(t-1)$, E_{BSmin}, $E_{\text{th\_max}}$
Output: $E_{\text{available}}(t)$, $E_{\text{outage}}(t)$
if $E_{\text{harvested}}(t), \ldots, E_{\text{harvested}}(t+x) > E_{\text{BSmin}}$ **then**
  Calculate $E_{\text{excess}}(t) = E_{\text{harvested}}(t) - E_{\text{consumed}}(t)$
  Update $E_{\text{available}}(t) = E_{\text{excess}}(t) + E_{\text{available}}(t-1)$
else if $E_{\text{harvested}}(t+n) < E_{\text{BSmin}}$ **and** $|E_{\text{available}}(t+n-1) - E_{\text{th\_max}}| > |E_{\text{harvested}}(t+n) - E_{\text{BSmin}}|$ **then**
  Set $E_{\text{consumed}}(t+n) = E_{\text{BSmin}}$
  Update $E_{\text{available}}(t+n) = E_{\text{available}}(t+n-1) - |E_{\text{harvested}}(t+n) - E_{\text{BSmin}}|$
else if $E_{\text{harvested}}(t) + \ldots + E_{\text{harvested}}(t+n-1) > n \cdot E_{\text{BSmin}}$ **then**
  Set $E_{\text{consumed}}(t), \ldots, E_{\text{consumed}}(t+n) = E_{\text{BSmin}}$
else
  Set $E_{\text{outage}}(t) = 1$
end if

Algorithm 4 Nighttime Operation (Solar-Aware)

Input: $E_{\text{consumed}}(t')$, $E_{\text{available}}(t'-1)$, E_{THmin}
Output: $E_{\text{available}}(t')$, $E_{\text{outage}}(t')$
if $E_{\text{consumed}}(t') - E_{\text{available}}(t'-1) \leq E_{\text{THmin}}$ **then**
  Update $E_{\text{available}}(t') = E_{\text{available}}(t'-1) - E_{\text{consumed}}(t')$
else
  Set $E_{\text{outage}}(t') = 1$
end if

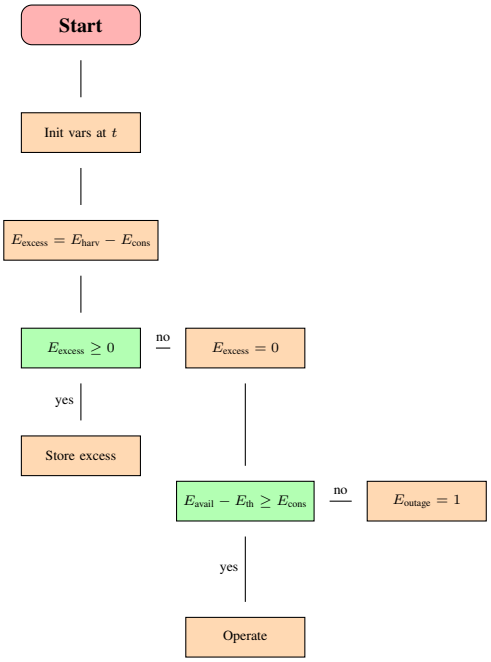

Fig. 6. Energy Outage Decision Algorithm in non-solar prediction model (Daytime Operation, business-as-usual)

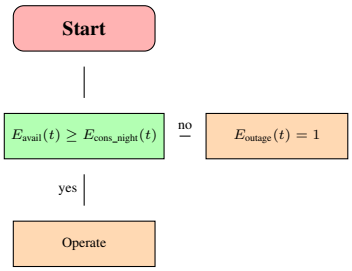

Fig. 7. Energy Outage Decision Algorithm in non-solar prediction model (Nighttime Operation, business-as-usual)

efficient energy utilization and system stability. The algorithm begins by assessing whether the cumulative harvested solar energy over a specified time window meets the minimum energy threshold required for BS operation. If so, any excess energy beyond the consumption needs is stored in the battery for later use. In cases where the cumulative harvested energy is insufficient to meet the minimum requirement, the algorithm intelligently adjusts the energy consumption based on the available energy and predictions of incoming energy. It aims to sustain essential operations by optimizing energy utilization while ensuring the battery's minimum threshold is not compromised. If neither of the above conditions is met, indicating a prolonged energy deficit, the algorithm activates a fallback mechanism. This mechanism ensures that the BS operates at the minimum required energy level for a predefined period, maintaining critical services while mitigating the risk of system failure. In scenarios where none of the conditions are satisfied, indicating an extended energy shortfall, the algorithm triggers an outage state. This state serves as a safety measure to prevent critical system failure and allows for necessary interventions or alternative power sources to be activated.

During the nighttime, when solar energy harvesting is not available, the algorithm manages the BS's operation by assessing the available energy in the battery from the previous

TABLE III
COND-LSTM VS. TRADITIONAL LSTM, TRANSFORMER AND MARKOV FOR A 48.94KW RATING PV PANEL.

Methods	nRMSE (H)↓ (%)	RMSE (H)↓ (W)	RMSE (D)↓ (W)	MAE (D)↓ (W)	ME (D)↓ (W)	MPE (D)↓ (%)
Markov	21.238	8588.413	120815.054	94364.946	-10471.987	52.811
LSTM	2.377	1043.646	9308.663	6990.764	2763.534	1.932
Transformer	1.480	648.136	12365.747	11448.602	-11087.669	-8.342
Cond-LSTM	**0.776**	**343.856**	**2795.262**	**2231.747**	**-108.615**	**-0.410**

time step. It ensures that the BS only operates within the constraints of available energy to prevent system instability or failure during periods of limited energy supply. If the energy consumed exceeds the available energy, indicating an energy deficit, the algorithm triggers an outage state to maintain system stability and prevent overload.

V. SIMULATION SETUP AND EVALUATIONS

A. Evaluation 1: Energy Harvesting Forecasting Methods

In this section, we evaluate the energy harvesting predictions made by a Cond-LSTM, vs. LSTM, Transformer and Markov models. Table III assesses the models' accuracy for a 48.94 kW panel through RMSE for hourly and daily predictions, as well as Mean Absolute Error (MAE), Mean Error (ME), and Mean Percentage Error (MPE) for daily energy harvesting predictions. The results quantify the error metrics in watts, where 'H' denotes hourly predictions and 'D' indicates daily estimates. An downward arrow signifies that lower values reflect superior predictive performance. The results reveal that the Cond-LSTM model significantly outperforms the other approaches. We used the same dataset for all models evaluated in this paper to ensure fairness. Variations in PV panel sizes and data lengths can significantly impact most error metrics. Normalized RMSE[2] (nRMSE) is provided for comparing with results from other papers, as this metric is not significantly affected by PV panel size or data length. Prior works found that LSTMs achieve 3.6% nRMSE with 600 epochs [61]. In comparison, our Cond-LSTM model achieves 0.78% nRMSE with a maximum of 500 epochs.

We also evaluated the LSTM and Cond-LSTM models using a time-series split to separate training and testing data across several partitions, which allows us to validate the model predictability across different scenarios. Data were partitioned four ways, with the training and test distributions set as 4 years/4 years, 8 years/4 years, 12 years/4 years, and 16 years/4 years. We applied the time-series split separately for data from four regions, assessing both RMSE and nRMSE for each. Fig. 8, depicting the time-series split for cross-validation across different regions, indicates that the Cond-LSTM outperforms the LSTM across all four datasets in all four regions.

B. Evaluation 2: Applicability to Different Regions

To assess how Cond-LSTM performance changes depending on local weather patterns, we selected several areas characterized by their distinct climatic features and trained a model for each location. We chose Rapid City in South Dakota (SD) (renowned for its unpredictable weather patterns [62]) to test the model's performance in a variable climate environment. Another two regions selected were: California (CA), representing the western United States, and Virginia (VA), reflecting the eastern United States. Similarly, for each location, 20

[2]nRMSE is defined as $nRMSE = RMSE/(A_{max} - A_{min})$, where A represents actual data

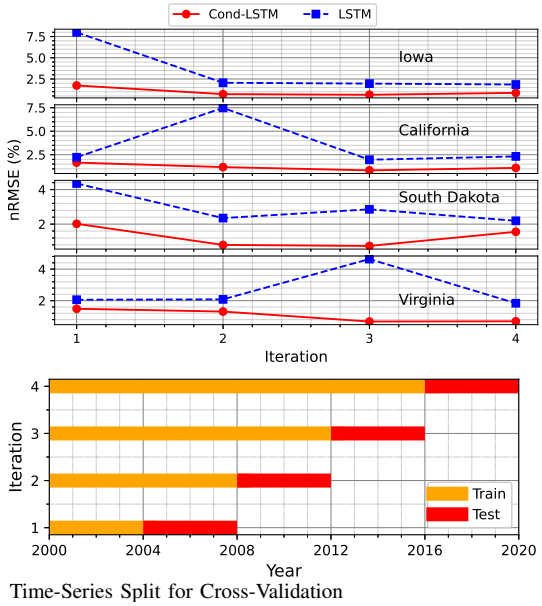

Fig. 8. Time-Series Split for Cross-Validation

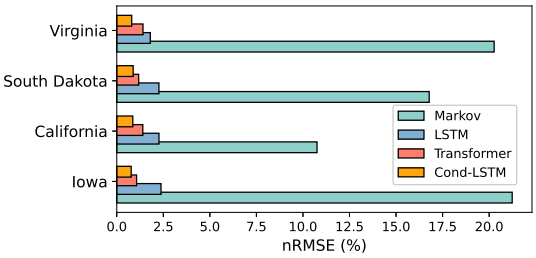

Fig. 9. nRMSE of Markov, LSTM, Transformer and Cond-LSTM

years of historical data are used for model development and 1 year of data for evaluation. Results show that the RMSE of the Cond-LSTM prediction for different regions still remain low even for a large size PV panel ($48.94kW$ DC rating). The RMSE of South Dakota was the highest, at $405.973W$. The RMSEs of all other locations are actually better ($4.39\% - 18.45\%$ improvement). The results shows that for all those regions, Cond-LSTM have a stabler and much more accurate prediction than Markov, LSTM and Transformer method. Fig. 9 presents the nRMSE (normalized by range) for the Markov, LSTM, Transformer and Cond-LSTM models across four distinct locations. LSTM, Transformer and Cond-LSTM models exhibit stability across varying weather conditions, in contrast to the Markov model, which exhibits instability across different datasets. Notably, the Cond-LSTM achieves the highest prediction accuracy, with an $nRMSE = 0.776\%, 0.861\%, 0.882\%, 0.802\%$ for Iowa, California, South Dakota and Virginia respectively. In addition, we investigate the model sizes of the three machine learning models, as shown in Table IV. Although the Transformer model achieves comparable accuracy, it has a significantly larger model size in terms of parameters, overall model size, and floating point operations per second (FLOPs). The proposed Cond-LSTM outperforms in both accuracy and resource efficiency, enabling more reliable and efficient repeated energy predictions for the resource allocation process.

C. Evaluation 3: Generalizability

In this section, we evaluate how well a model trained for one location can perform at a new location without re-training.

TABLE IV
RESOURCE CONSUMPTION OF DIFFERENT MODELS

Methods	Parameter size↓	Model size↓	FLOPs ↓
LSTM	5793	22.63 KB	135936
Transformer	118081	461.25 KB	4889088
Cond-LSTM	**5665**	**22.13 KB**	**398592**

TABLE V
OPTIMAL SIZING AND COST OF A GENERAL MODEL APPLIED TO SOUTH DAKOTA, CALIFORNIA AND VIRGINIA REGIONS

Harvesting Data	Number of PV Panel Modules	Number of Battery Modules	Cost Difference ↓
Location	South Dakota		
Ground Truth	57	21	0 ($57881.31)
LSTM	58	23	7.655%
Transformer	58	22	4.039%
Cond-LSTM	57	21	**0%**
Location	California		
Ground Truth	50	22	0 ($58265.14)
LSTM	51	21	3.174%
Transformer	55	22	2.096%
Cond-LSTM	51	22	**0.419%**
Location	Virginia		
Ground Truth	86	35	0 ($94270.87)
LSTM	86	32	6.662%
Transformer	87	36	2.480%
Cond-LSTM	86	35	**0%**

We trained a general model by using 2000 - 2019 data from the Iowa region, and then used the pre-trained model to predict the 2020 year harvesting data for locations in California, South Dakota and Virginia. The ability to use a pre-trained model helps avoid the financial and environmental costs of re-training a model for every new location.

The nRMSE (normalized by range) of the general model's prediction for those regions are 2.624%, 2.010%, 1.162%, respectively. Compared to the Cond-LSTM models trained specifically for a region, a non-conditional LSTM trained on local data has a $0.999\% - 1.406\%$ nRMSE difference, while Markov based on the same data has an $9.895\% - 19.466\%$ nRMSE difference. The general Cond-LSTM model, however, only shows $0.360\% - 1.763\%$ nRMSE difference, which is similar to the accuracy of LSTMs specifically trained on the local data. These results extend beyond the specific case of a model trained on Iowa being evaluated in other locations. If the model is trained solely on data from CA, SD or VA, and then evaluated in new locations, the results are similar: the 'general' model only has an 2.9% increase in nRMSE, on average. This shows that a Cond-LSTM model trained in one place can predict the harvesting energy of other locations with high accuracy.

Table V presents the PV/battery numbers and associated costs obtained using a model that makes predictions in new locations. Additionally, we compare the performance of Cond-LSTM, Transformer (generalized), and LSTM (generalized) models, demonstrating that the Cond-LSTM predictions closely match the ground truth. This indicates that a model trained with data from one location can still accurately predict the size of a solar-powered system in another. Furthermore, when provisioning for new locations—particularly those with insufficient historical weather data for effective training or no solar harvesting data—short-term weather data can be used effectively by leveraging a well-trained model from regions with abundant historical weather and harvesting data.

D. Evaluation 4: Sizing the Solar System and Cost

The results in Table VI indicate that the Markov models exhibit significant errors in estimating the size of solar-powered systems. Although the LSTM model and Transformer yields good results, the Cond-LSTM model outperforms both. However, this marginal discrepancy between the LSTM, Transformer and Cond-LSTM models can be attributed to the low DC rating (0.43 kW) used for a single PV panel module. The benefits of our algorithm become more pronounced when using larger PV panels or custom-designed integrated panels. As the size of each panel grows, over or under provisioning by a single panel can cause the error to amplify in size due to the increased power per PV panel. This will lead to considerable increases in RMSE for the non Cond-LSTM approaches, as demonstrated in Table III.

TABLE VI
OPTIMAL SOLAR SIZING/COST PER DIFFERENT PREDICTION MODELS

Harvesting Data	Number of PV Panel Modules	Number of Battery Modules	Cost Difference ↓
Ground Truth	48	22	0 ($57776.70)
Markov	69	19	1.993%
LSTM	50	22	0.845%
Transformer	49	23	4.046%
Cond-LSTM	47	22	**0.423%**

E. Evaluation 5: User Power Allocation

The solution of objective optmization function in formula (6) provides the power allocated to each user in each interval. These allocations represent the optimized strategy for maximizing the network's cumulative SNR under the given constraints. The results are then analyzed to assess network performance and adherence to energy limitations. To evaluate the effectiveness of our proposed power allocation strategy in a cellular network, we conducted a simulation using MATLAB. The objective was to maximize the cumulative SNR over a one-hour period, with power allocation decisions made every 60 seconds. This resulted in a total of 60 intervals. The simulation parameters were set as follows:

- Number of users (`numUsers`): 5
- Number of intervals (`numIntervals`): 60 (corresponding to 1 hour with decisions every 60 seconds)
- Channel gain parameters: Mean (`mu_g`) = 1, Standard deviation (`sigma_g`) = 0.2
- Idle power per interval (`P0`): 10 Watts
- Constant energy budget per interval (`constantEnergyBudgetPerInterval`): 100
- Normalized noise power (`sigma2`): 1
- Bandwidth (`BW`): 20 MHz
- Maximum allowable power (`P_max`): 20 Watts

The choice of $P_{\max}$ in our simulation or optimization problem is context-dependent. While the provided article mentions a 4-port MIMO and dual-band radio delivering 4x40 W of radiofrequency power, the consumption of 1060 W encompasses the entire radio unit, including signal processing and other operational aspects. More explanation added below. The choice of $P_{\max}$ in our simulation or optimization problem is context-dependent. In our scenario, $P_{\max}$ is determined based on hardware constraints, regulatory limits, and the desired trade-off between power consumption and performance. For instance, a $P_{\max}$ of 20 Watts may be realistic for a small-scale BS with limited power capabilities.

Stochastic channel gains were generated for each user and each interval, based on the specified mean and standard deviation. MATLAB's `fmincon` function was used to solve the nonlinear optimization problem. The objective function was

designed to maximize the cumulative SNR, and the constraints ensured that power allocations did not exceed the available energy budget and adhered to the maximum power limits. The optimization process yielded power allocations for each user at every interval over the one-hour period. To visualize these results, a time-series plot was generated, showing the power allocated to each user over time. The time-series plot in Fig. 10 provides a detailed view of how the power allocation strategy varied across different intervals for each user. It revealed patterns in power distribution and highlighted periods where certain users were allocated more power, possibly due to better channel conditions or lower interference.

Simulation results demonstrate the effectiveness of our optimization approach in dynamically allocating power to maximize SNR. The time-series plot, in particular, offers valuable insights into the allocation strategy, indicating how the network adapts to varying conditions and user demands over time. This approach not only enhances network performance but also ensures efficient utilization of energy resources.

F. Evaluation 6: Comparison of Outage in Non-Solar Aware and Proposed Solar Aware Scenarios

In this section, we compare the outage percentages between the non-solar aware and proposed solar prediction scenarios which can be seen in Fig. 11.

We conducted simulations using both the non-solar aware and solar aware algorithms and analyzed the outage percentages during the daytime and nighttime operations.

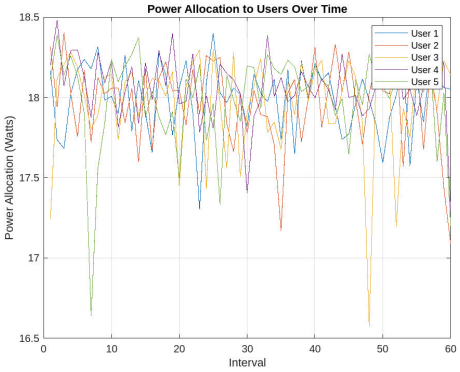

Fig. 10. Time-series plot of the power allocated to each user in the cell

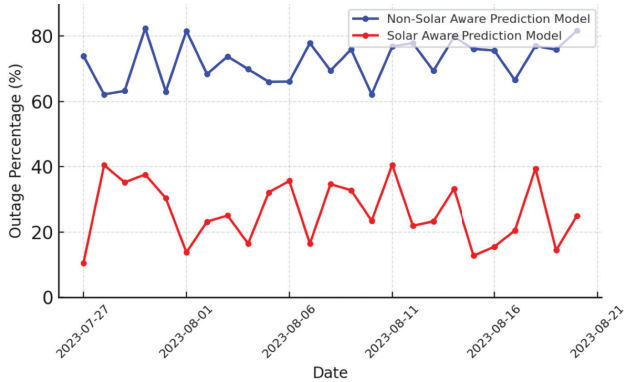

Fig. 11. Comparison of Outage in Non-Solar Aware and Proposed Solar Aware Prediction Scenarios

We model a solar energy harvesting system, comprising a PV panel with DC rating 1 KW. We assume that 12 V, 205 Ah flooded lead acid batteries are used. The simulation spans from July 27th, 2024, to August 20th, 2024, encompassing 25 days

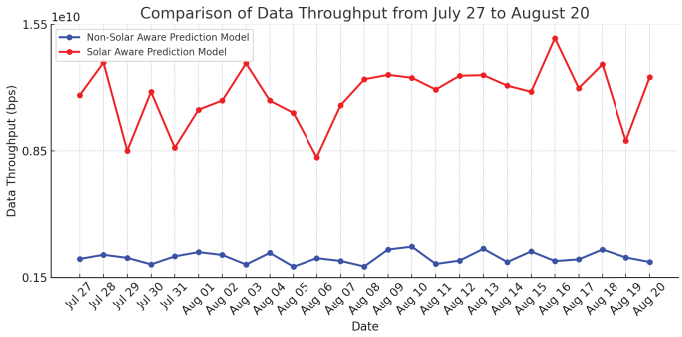

Fig. 12. Comparison of data throughput in Non-Solar Aware and Proposed Solar Aware Prediction Scenarios

of operation. Energy management algorithms are evaluated under two scenarios: the Non Prediction Algorithm, which reacts solely to real-time energy availability and demand, and the proposed Solar Prediction Algorithm, which utilizes a predictive LSTM model to anticipate future solar energy availability. Outage detection thresholds are set at 100 kWh for high-demand situations and 20 kWh for low battery conditions. Key performance metric, energy outage percentage, provides insights into the system's operational efficacy. Simulations are conducted using MATLAB R2024a, leveraging realistic solar energy data and algorithmic implementations to evaluate system performance comprehensively.

G. Evaluation 7: Comparison of Throughput in Non-Prediction and Proposed Prediction Scenarios

Throughput refers to the amount of data transferred successfully over a network within a given period. The range for data throughput can vary significantly depending on the specific context and application of the BS like network technology, channel conditions (including factors such as signal strength, interference and noise), bandwidth allocation, number of users, QoS Requirements, equipment and configuration.

Throughput can be calculated using following formula:

$$\begin{aligned}\text{Throughput} = &\frac{\text{Bandwidth} \times \text{MCS} \times \text{N spatial streams}}{\text{Number of bits per byte}} \\ &\times \text{N symbols per subframe} \\ &\times \text{N subframes per millisecond}\end{aligned} \tag{16}$$

Channel bandwidth is expressed in hertz (Hz). MCS (Modulation and Coding Scheme) determines the number of bits transmitted per symbol and the error correction capability of the modulation scheme. Number of spatial streams represents the number of independent data streams transmitted simultaneously using multiple antennas (MIMO - Multiple Input Multiple Output). Number of symbols per subframe refers to the number of modulation symbols transmitted in each subframe. Number of subframes per millisecond indicates the frequency of subframe transmissions within one millisecond. Number of bits per byte represents the number of bits in a byte (usually 8 bits).

Comparison of data throughput in Non-Solar Aware and Proposed Solar Aware Prediction Scenarios can be seen in Fig. 12 which proves the effectiveness of proposed model in increasing the throughput of the system. As it can be seen from the figure, for the same battery configuration, our algorithm

achieves 8 billion bps greater data throughput than a non-solar aware approach.

VI. Conclusions and Future Work

In this paper, we presented a novel system model for integrating photovoltaic (PV) technology to power BSs in a 5G network, ensuring continuous operation through efficient energy management.

We introduced an accurate forecasting approach, the Cond-LSTM, designed to optimize the deployment of solar-powered macro BS. Our model demonstrated versatility across various geographic regions, highlighting its broad applicability. Our comparative analysis showed that the Cond-LSTM model outperformed Markov, LSTM and Transformer models in key error metrics such as RMSE, MAE, ME, and MPE.

Our optimization approach for power allocation within the cellular network further demonstrated the system's ability to maximize SNR while adhering to energy constraints. By incorporating real-time traffic data and utilizing advanced optimization techniques, we ensured efficient energy utilization, minimized outages, and enhanced overall network performance.

By simulating scenarios that closely mirror the energy consumption patterns of macro 5G BSs and a given tolerable power outage rate, we determined the number of PV panel modules and battery modules required for a solar-powered 5G base BS. The results showed that our model closely aligned with ground-truth data, enabling precise determination of the required quantities of PV panels and storage batteries. Additionally, we demonstrated that our model, once trained on data from a single region, could effectively forecast solar-powered system outputs and inform sizing decisions in various other regions.

Future work will focus on extending the model to encompass more complex scenarios, such as varying environmental conditions and dynamic user demands, and exploring the integration of additional renewable energy sources to further enhance the reliability and efficiency of solar-powered BSs.

References

[1] R. Swanepoel D. J. Ludick and W. Barnard, "Efficient simulation of 5g mobile base station antennas for rf safety analysis," *2022 International Conference on Electromagnetics in Advanced Applications (ICEAA)*, pp. 317–317, 2022.

[2] H. Bogucka and O. Holland, "Multi-layer approach to future green mobile communications," *IEEE Intelligent Transportation Systems Magazine*, vol. 5, no. 4, pp. 28–37, 2013.

[3] G. Ye, "Research on reducing energy consumption cost of 5g base station based on photovoltaic energy storage system," *2021 IEEE International Conference on Computer Science, Electronic Information Engineering and Intelligent Control Technology (CEI)*, pp. 480–484, 2021.

[4] R. Clark., "Network operators focus on energy savings as costs soar," *https://www.lightreading.com/network-operators-focus-on-energy-savings-as-costs-soar/d/d-id/781453/ (accessed Jan. 11, 2022)*, 2022.

[5] "Is telco sustainability a priority or challenge?," *accessed on May. 15, 2022. [Online]. Available: https://www.sdxcentral.com/articles/news/is-telco-sustainability-a-priority-or-challenge/2022/05/*, 2022.

[6] "Global system mobile association (gsma)," *accessed on Nov. 5, 2015. [Online]. Available: http://www.gsma.com/*, 2015.

[7] Dulip Tillekeratne, M Wilson, and L Purnell, "Renewable energy for mobile towers: opportunities for low-and middle-income countries," *Global System Mobile Association (GSMA), Tech. Rep*, 2020.

[8] S. Naderi, K. Bundy, T. Whitney, A. Abedi, A. Weiskittel, and A. Contosta, "Sharing wireless spectrum in the forest ecosystems using artificial intelligence and machine learning," *International Journal of Wireless Information Networks*, vol. 29, no. 3, pp. 257–268, 2022.

[9] S. Naderi, S. Khosroazad, and A. Abedi, "Relay-assisted wireless energy transfer for efficient spectrum sharing in harsh environments," *International Journal of Wireless Information Networks*, vol. 29, no. 3, pp. 240–249, 2022.

[10] M. Marsan et. al., "Towards zero grid electricity networking: Powering bss with renewable energy sources," *Proc. IEEE ICC*, June 2013.

[11] Ankur Vora and Kyoung-Don Kang, "Effective 5g wireless downlink scheduling and resource allocation in cyber-physical systems," *Technologies*, vol. 6, pp. 105, 11 2018.

[12] Marco Miozzo, Davide Zordan, Paolo Dini, and Michele Rossi, "Solarstat: Modeling photovoltaic sources through stochastic markov processes," in *2014 IEEE International Energy Conference (ENERGYCON)*. IEEE, 2014, pp. 688–695.

[13] Vinay Chamola and Biplab Sikdar, "Resource provisioning and dimensioning for solar powered cellular base stations," in *2014 IEEE Global Communications Conference*. IEEE, 2014, pp. 2498–2503.

[14] Vinay Chamola and Biplab Sikdar, "Outage estimation for solar powered cellular base stations," in *2015 IEEE ICC*, 2015, pp. 172–177.

[15] Praveen Gorla and Vinay Chamola, "Battery lifetime estimation for energy efficient telecommunication networks in smart cities," *Sustainable Energy Technologies and Assessments*, vol. 46, pp. 101205, 2021.

[16] Amandeep Sharma and Ajay Kakkar, "A review on solar forecasting and power management approaches for energy-harvesting wireless sensor networks," *International Journal of Communication Systems*, vol. 33, no. 8, pp. e4366, 2020.

[17] S Viswanatha Rao, Sakuntala S Pillai, and G Shiny, "Enhancing the performance of an energy harvesting wireless sensor node using markov decision process," in *Advances in Electrical and Computer Technologies: Select Proceedings of ICAECT 2020*. Springer, 2021, pp. 581–593.

[18] S Dharmaraja, Anisha Aggarwal, and Kamlesh Naresa, "Analytical modelling and simulation of drx mechanism for energy harvesting," in *2022 Annual Reliability and Maintainability Symposium (RAMS)*. IEEE, 2022, pp. 1–5.

[19] Muhammad Faizan Ghuman, Adnan Iqbal, Hassaan Khaliq Qureshi, and Marios Lestas, "Asim: Solar energy availability model for wireless sensor networks," in *Proceedings of the 3rd International Workshop on Energy Harvesting & Energy Neutral Sensing Systems*, 2015, pp. 21–26.

[20] Steven D Miller, Matthew A Rogers, John M Haynes, Manajit Sengupta, and Andrew K Heidinger, "Short-term solar irradiance forecasting via satellite/model coupling," *Solar Energy*, vol. 168, pp. 102–117, 2018.

[21] Vishal Sharma, Dazhi Yang, Wilfred Walsh, and Thomas Reindl, "Short term solar irradiance forecasting using a mixed wavelet neural network," *Renewable Energy*, vol. 90, pp. 481–492, 2016.

[22] Mingming Gao, Jianjing Li, Feng Hong, and Dongteng Long, "Day-ahead power forecasting in a large-scale photovoltaic plant based on weather classification using lstm," *Energy journal*, vol. 187, pp. 115838, 2019.

[23] Xiangyun Qing and Yugang Niu, "Hourly day-ahead solar irradiance prediction using weather forecasts by lstm," *Energy*, vol. 148, pp. 461–468, 2018.

[24] Navin Sharma, Pranshu Sharma, David Irwin, and Prashant Shenoy, "Predicting solar generation from weather forecasts using machine learning," in *2011 IEEE international conference on smart grid communications (SmartGridComm)*. IEEE, 2011, pp. 528–533.

[25] Mohammad Safayet Hossain and Hisham Mahmood, "Short-term photovoltaic power forecasting using an lstm neural network and synthetic weather forecast," *Ieee Access*, vol. 8, pp. 172524–172533, 2020.

[26] Chun-Hung Liu, Jyh-Cherng Gu, and Ming-Ta Yang, "A simplified lstm neural networks for one day-ahead solar power forecasting," *Ieee Access*, vol. 9, pp. 17174–17195, 2021.

[27] Su-Chang Lim, Jun-Ho Huh, Seok-Hoon Hong, Chul-Young Park, and Jong-Chan Kim, "Solar power forecasting using cnn-lstm hybrid model," *Energies*, vol. 15, no. 21, pp. 8233, 2022.

[28] Yu-Jen Ku, Sandalika Sapra, Sabur Baidya, and Sujit Dey, "State of energy prediction in renewable energy-driven mobile edge computing using cnn-lstm networks," in *2020 IEEE Green Energy and Smart Systems Conference (IGESSC)*. IEEE, 2020, pp. 1–7.

[29] Hua Han, Hongyi Liu, Xiaoyun Zuo, Guangze Shi, Yao Sun, Zhangjie Liu, and Mei Su, "Optimal sizing considering power uncertainty and power supply reliability based on lstm and mopso for swpbms," *IEEE Systems Journal*, vol. 16, no. 3, pp. 4013–4023, 2022.

[30] A Vaswani, "Attention is all you need," *Advances in Neural Information Processing Systems*, 2017.
[31] Elham M Al-Ali, Yassine Hajji, Yahia Said, Manel Hleili, Amal M Alanzi, Ali H Laatar, and Mohamed Atri, "Solar energy production forecasting based on a hybrid cnn-lstm-transformer model," *Mathematics*, vol. 11, no. 3, pp. 676, 2023.
[32] Jiří Pospíchal, Martin Kubovčík, and Iveta Dirgová Luptáková, "Solar irradiance forecasting with transformer model," *Applied Sciences*, vol. 12, no. 17, pp. 8852, 2022.
[33] Miguel López Santos, Xela García-Santiago, Fernando Echevarría Camarero, Gonzalo Blázquez Gil, and Pablo Carrasco Ortega, "Application of temporal fusion transformer for day-ahead pv power forecasting," *Energies*, vol. 15, no. 14, pp. 5232, 2022.
[34] Muhammad Munsif, Min Ullah, U Fath, Samee Ullah Khan, Noman Khan, and Sung Wook Baik, "Ct-net: A novel convolutional transformer-based network for short-term solar energy forecasting using climatic information.," *Computer Systems Science & Engineering*, vol. 47, no. 2, 2023.
[35] Kian Long Tan, Chin Poo Lee, Kalaiarasi Sonai Muthu Anbananthen, and Kian Ming Lim, "Roberta-lstm: a hybrid model for sentiment analysis with transformer and recurrent neural network," *IEEE Access*, vol. 10, pp. 21517–21525, 2022.
[36] Feyza Duman Keles, Pruthuvi Mahesakya Wijewardena, and Chinmay Hegde, "On the computational complexity of self-attention," in *International Conference on Algorithmic Learning Theory*. PMLR, 2023, pp. 597–619.
[37] Yekun Ke, Yingyu Liang, Zhenmei Shi, Zhao Song, and Chiwun Yang, "Curse of attention: A kernel-based perspective for why transformers fail to generalize on time series forecasting and beyond," *arXiv preprint arXiv:2412.06061*, 2024.
[38] Yi Yu, Abhishek Srivastava, and Simon Canales, "Conditional lstm-gan for melody generation from lyrics," *ACM Transactions on Multimedia Computing, Communications, and Applications (TOMM)*, vol. 17, no. 1, pp. 1–20, 2021.
[39] Tsung-Hsien Wen, Milica Gasic, Nikola Mrksic, Pei-Hao Su, David Vandyke, and Steve Young, "Semantically conditioned lstm-based natural language generation for spoken dialogue systems," *arXiv preprint arXiv:1508.01745*, 2015.
[40] Zhigang Xie, Xin Song, Jing Cao, and Siyang Xu, "Energy efficiency task scheduling for battery level-aware mobile edge computing in heterogeneous networks," *ETRI Journal*, vol. 44, no. 5, pp. 746–758, 2022.
[41] San Kim and Jinyeong Lee, "Optimal scheduling strategy for distribution network with mobile energy storage system and offline control pvs to minimize the solar energy curtailment," *Energies*, vol. 17, no. 9, pp. 2234, 2024.
[42] Bin Huang and Jianhui Wang, "Deep-reinforcement-learning-based capacity scheduling for pv-battery storage system," *IEEE Transactions on Smart Grid*, vol. 12, no. 3, pp. 2272–2283, 2020.
[43] Yuyi Mao, Yaming Luo, Jun Zhang, and Khaled B. Letaief, "Energy harvesting small cell networks: feasibility, deployment, and operation," *IEEE Communications Magazine*, vol. 53, no. 6, pp. 94–101, 2015.
[44] Juhyun Lee and Jae Hong Lee, "Performance analysis and resource allocation for cooperative d2d communication in cellular networks with multiple d2d pairs," *IEEE Communications Letters*, vol. 23, no. 5, pp. 909–912, 2019.
[45] Sree Krishna Das, Md Siddikur Rahman, Lina Mohjazi, Muhammad Ali Imran, and Khaled M Rabie, "Reinforcement learning-based resource allocation for m2m communications over cellular networks," in *2022 IEEE Wireless Communications and Networking Conference (WCNC)*. IEEE, 2022, pp. 1473–1478.
[46] Suhare Solaiman, Laila Nassef, and Etimad Fadel, "User clustering and optimized power allocation for d2d communications at mmwave underlaying mimo-noma cellular networks," *IEEE Access*, vol. 9, pp. 57726–57742, 2021.
[47] Ke Wang, Wei Heng, Jinming Hu, Xiang Li, and Jing Wu, "Energy-efficient resource allocation for energy harvesting-powered d2d communications underlaying cellular networks," in *2018 IEEE 88th Vehicular Technology Conference (VTC-Fall)*, 2018, pp. 1–5.
[48] N M d Bilal and T. Velmurugan, "A review of efficient resource allocation for mm-wave d2d communication in cellular networks using ml algorithm," in *2023 3rd International Conference on Pervasive Computing and Social Networking (ICPCSN)*, 2023, pp. 1307–1312.
[49] G. Vallero, D. Renga, M. Meo, and M. A. Marsan, "Greener ran operation through machine learning," *IEEE Transactions on Network and Service Management*, vol. 16, no. 3, pp. 896–908, Sept. 2019.
[50] N. Piovesan, D. López-Pérez, M. Miozzo, and P. Dini, "Joint load control and energy sharing for renewable powered small base stations: A machine learning approach," *IEEE Transactions on Green Communications and Networking*, vol. 5, no. 1, pp. 512–525, March 2021.
[51] Nicola Piovesan, Angel Fernandez Gambin, Marco Miozzo, Michele Rossi, and Paolo Dini, "Energy sustainable paradigms and methods for future mobile networks: A survey," *Computer Communications*, vol. 119, pp. 101–117, 2018.
[52] Jumaboev Sherozbek, Jaewoo Park, Mohammad Shaheer Akhtar, and O-Bong Yang, "Transformers-based encoder model for forecasting hourly power output of transparent photovoltaic module systems," *Energies*, vol. 16, no. 3, pp. 1353, 2023.
[53] "Weather Data - System Advisor Model - SAM.," .
[54] "PySAM — NREL-PySAM 5.1.0 documentation," .
[55] Shuodi Hui, Huandong Wang, Tong Li, Xinghao Yang, Xing Wang, Junlan Feng, Lin Zhu, Chao Deng, Pan Hui, Depeng Jin, et al., "Large-scale urban cellular traffic generation via knowledge-enhanced gans with multi-periodic patterns," in *Proceedings of the 29th ACM SIGKDD Conference on Knowledge Discovery and Data Mining*, 2023, pp. 4195–4206.
[56] Linda Hardesty, "5g base stations use a lot more energy than 4g base stations: Mtn," *Fierce Wireless*, vol. 3, 2020.
[57] Feng Zhou, Jie Chen, Guoyuan Ma, and Zhongliang Liu, "Energy-saving analysis of telecommunication base station with thermosyphon heat exchanger," *Energy and Buildings*, vol. 66, pp. 537–544, 2013.
[58] Deepti Sharma, Sanyam Singhal, Amrita Rai, and Amandeep Singh, "Analysis of power consumption in standalone 5g network and enhancement in energy efficiency using a novel routing protocol," *Sustainable Energy, Grids and Networks*, vol. 26, pp. 100427, 2021.
[59] Mohammed W Baidas, Rola W Hasaneya, Rashad M Kamel, and Sultan Sh Alanzi, "Solar-powered cellular base stations in kuwait: A case study," *Energies*, vol. 14, no. 22, pp. 7494, 2021.
[60] Theodore Rappaport, *Wireless Communications: Principles and Practice*, Prentice Hall PTR, USA, 2nd edition, 2001.
[61] Chibuzor N Obiora, Ahmed Ali, and Ali N Hasan, "Forecasting hourly solar irradiance using long short-term memory (lstm) network," in *2020 11th International Renewable Energy Congress (IREC)*. IEEE, 2020, pp. 1–6.
[62] Nate Silver and Reuben Fischer-Baum, "Which city has the most unpredictable weather?," Dec. 2014.

BIOGRAPHY

Sonia Naderi received her Ph.D. in Electrical Engineering and subsequently completed a postdoctoral fellowship at the University of California, Santa Cruz. Her research interests lie in wireless communications, with a focus on sustainable wireless communication system design. She is currently an assistant professor at Los Angeles Valley College and an adjunct faculty member at Loyola Marymount University, Los Angeles.

Yawen Guo is currently pursuing a Ph.D. in Electrical and Computer Engineering at UC Santa Cruz. Her research focuses on applying machine learning to green communication systems and Visible Light Communication to enhance energy efficiency and drive innovative technology integration in the field of communication. She is passionate about sustainability and is dedicated to developing solutions that advance communication technologies while minimizing environmental impact.

Colleen Josephson is an Assistant Professor of Electrical and Computer Engineering at UC Santa Cruz, where her research focuses on wireless sensing systems to enable and improve sustainable practices. Prior to joining UC Santa Cruz, Dr. Josephson was a research scientist at VMware, leading working groups in the Next G Alliance focused on societal and environmental impact. She completed her PhD in Electrical Engineering at Stanford University, and received S.B and MEng degrees from the Massachusetts Institute of Technology.